Phase Diagram for the Winfree Model of Coupled Nonlinear Oscillators

Joel T. Ariaratnam and Steven H. Strogatz
Center for Applied Mathematics, Cornell University, Ithaca, New York 14853
(Received 11 December 2000)

In 1967 Winfree proposed a mean-field model for the spontaneous synchronization of chorusing crickets, flashing fireflies, circadian pacemaker cells, or other large populations of biological oscillators. Here we give the first bifurcation analysis of the model, for a tractable special case. The system displays rich collective dynamics as a function of the coupling strength and the spread of natural frequencies. Besides incoherence, frequency locking, and oscillator death, there exist hybrid solutions that combine two or more of these states. We present the phase diagram and derive several of the stability boundaries analytically.

DOI: 10.1103/PhysRevLett.86.4278 PACS numbers: 05.45.Xt, 87.10.+e

The collective behavior of limit-cycle oscillators was first investigated by Winfree [1]. Using a mean-field model of coupled phase oscillators with distributed natural frequencies, he discovered that collective synchronization is a threshold phenomenon, the temporal analog of a phase transition. Specifically, when the strength of the coupling exceeds a critical value, some oscillators spontaneously synchronize to a common frequency, overcoming the disorder in their natural frequencies. The model was subsequently refined by Kuramoto [2] and others [3,4], with applications to Josephson junction arrays [5], neutrino flavor oscillations [6], Brownian ratchets [7], bubbly fluids [8], semiconductor laser arrays [9], and Landau damping of plasmas [10]. Despite all the activity that Winfree's work ultimately provoked, surprisingly little is known about the dynamics of his original model. The problem is that his model has been difficult to analyze mathematically, at least in its most general form.

In this Letter, we identify a special case of the model which can be solved exactly. This version of the model is also related to recent work on pulse-coupled oscillators (where the oscillators interact by firing sudden impulses), a case of interest in neurobiology [11]. However, our motivation is more mathematical than biological. The goal is to understand the collective behavior and bifurcations of the model as a function of two parameters, the coupling strength and the spread of natural frequencies.

In the limit of weak coupling and nearly identical frequencies, our system reduces to the Kuramoto model, whose behavior is well understood [2–4]: it displays locked, partially locked, or incoherent states, depending on the choice of parameters. Away from this familiar regime, we find several hybrid states corresponding to various mixtures of locking, incoherence, and oscillator death (a cessation of oscillation caused by excessively strong coupling [12]).

The Winfree model is

$$\dot{\theta}_i = \omega_i + \frac{\kappa}{N} \sum_{j=1}^{N} P(\theta_j) R(\theta_i), \qquad (1)$$

for $i = 1, \ldots, N$, where $N \gg 1$. Here $\theta_i(t)$ is the phase of the ith oscillator at time t, $\kappa \geq 0$ is the coupling strength, and the frequencies ω_i are sampled from a symmetric unimodal probability density $g(\omega)$. We assume that the mean of $g(\omega)$ equals 1, by a suitable rescaling of time, and that its width is characterized by a parameter γ. The jth oscillator makes its presence felt through an influence function $P(\theta_j)$. In turn, the ith oscillator responds to the mean field (the average influence of the whole population) according to a sensitivity function $R(\theta_i)$.

From now on we consider the special case where

$$P(\theta) = 1 + \cos\theta, \qquad R(\theta) = -\sin\theta. \qquad (2)$$

Note that this $P(\theta)$ is a smooth but pulselike function. (At the end of this paper we consider a much more sharply peaked $P(\theta)$; then $\theta = 0$ represents the phase when the oscillator suddenly fires.) The specific form of $R(\theta)$ is chosen for its mathematical tractability. It is also consistent with the qualitative shape of the phase-response curve of some biological oscillators. For instance, the flashing rhythm of the firefly *Pteroptyx cribellata* [13] and the circadian rhythm of eclosion for *Drosophila* [14] show roughly sinusoidal resetting when subjected to weak light pulses [15]. With these choices, Eq. (1) becomes an idealized model for a population of pulse-coupled biological oscillators. The unusual aspect is that the coupling is through the phase-response curve [16], so that an oscillator can be either advanced or delayed by a pulse from another oscillator, depending on its phase when it receives the stimulus. This differs from the strictly excitatory or inhibitory coupling often used in integrate-and-fire models of neural oscillators.

We begin by describing our numerical simulations. Equation (1) was integrated numerically using $N = 800$ oscillators. The frequencies ω_i were chosen to be evenly spaced in the interval $I = [1 - \gamma, 1 + \gamma]$, corresponding to a uniform density $g(\omega) = 1/2\gamma$ for $\omega \in I$, and $g(\omega) = 0$ otherwise. The long-term behavior of the system was always found to be independent of the initial conditions.

 0031-9007/01/86(19)/4278(4)$15.00

To compare the long-term dynamics of individual oscillators, we compute the average frequency (also known as the rotation number) of each oscillator, $\rho_i = \lim_{t\to\infty}\theta_i(t)/t$. In our simulations, the limit was typically well approximated by integrating the system for 500 time units, starting from a random initial condition, although longer runs were sometimes necessary. The rotation numbers provide a useful measure of synchronization: two or more oscillators are frequency locked if they have the same rotation number.

Figure 1 plots ρ_i as a function of ω_i for increasing values of γ, at a fixed κ. For small γ, all the oscillators are locked [Fig. 1(a)]. They can be visualized as a pack of particles rotating at the same average rate around the unit circle, where $\theta_i(t)$ denotes the angular position of the ith oscillator. As γ is increased past a critical threshold, the coupling is no longer sufficient to keep all oscillators mutually entrained. Just above threshold, the system stays partially locked, with the fastest oscillators peeling away from the pack, but drifting incoherently relative to one another [Fig. 1(b)]. With further increases in γ, successively more oscillators peel away until eventually the entire population is incoherent [Fig. 1(c)]. For sufficiently large γ, the system converges to a state of partial death in which the slowest oscillators stop moving altogether, while the faster ones remain incoherent [Fig. 1(d)].

Partial locking and partial death are hybrid states. The two distinct branches in their rotation number plots [Figs. 1(b) and 1(d)] correspond to qualitatively different dynamics. We have also observed hybrid states with three and four branches [Fig. 2]. These more complicated states should all be regarded as variants of partial locking, since there is at least one branch of locked oscillators in each case. (Note that all these states are near each other in parameter space.) We label them according to their branches, as follows.

Locked-slipping-locked [Fig. 2(a)].—There are two separate plateaus of locked oscillators, at close to 2:1 frequency ratio in the example shown, separated by a branch of slipping oscillators. A slipping oscillator typically corotates with a locked group for several periods, then slips away for a few cycles before eventually rejoining the same group and repeating the pattern. Oscillators slip more or less frequently depending on their native frequency ω_i.

Slipping-locked-incoherent [Fig. 2(b)].—There is a central group of locked oscillators, flanked by slower ones that slip and faster ones that drift monotonically.

Quivering-slipping-locked-incoherent [Fig. 2(c)].—This state exists near partial death. It is similar to the state in Fig. 2(b), but with an added mode of behavior: the slowest oscillators quiver about their nearby death phases. An oscillator that quivers has zero rotation number—it remains trapped in the neighborhood of a single phase for all time—and hence is effectively dead, although not completely motionless. Figure 3 summarizes the system's long-term behavior as a function of κ and γ.

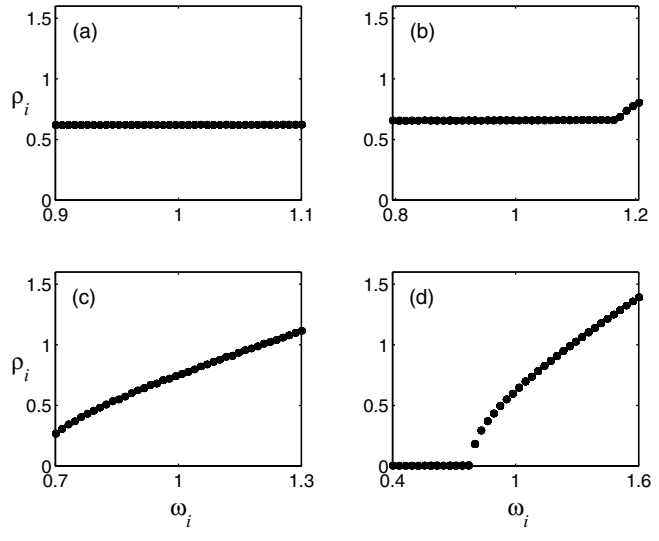

FIG. 1. Collective states, as indicated by rotation numbers, for $\kappa = 0.65$. Equation (1) with $P(\theta)$, $R(\theta)$ as in (2) was integrated for 500 time units starting from a random initial condition. (a) $\gamma = 0.1$: locking. (b) $\gamma = 0.205$: partial locking. (c) $\gamma = 0.3$: incoherence. (d) $\gamma = 0.6$: partial death.

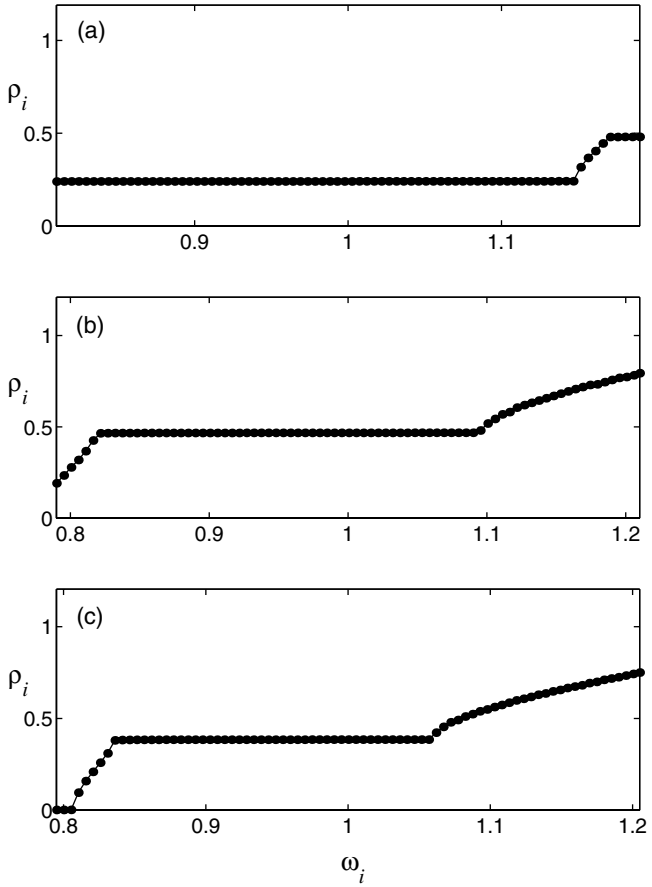

FIG. 2. Partially locked hybrid states. (a) $\gamma = 0.19$, $\kappa = 0.78$: locked-slipping-locked. (b) $\gamma = 0.21$, $\kappa = 0.76$: slipping-locked-incoherent. (c) $\gamma = 0.205$, $\kappa = 0.79$: quivering-slipping-locked-incoherent.

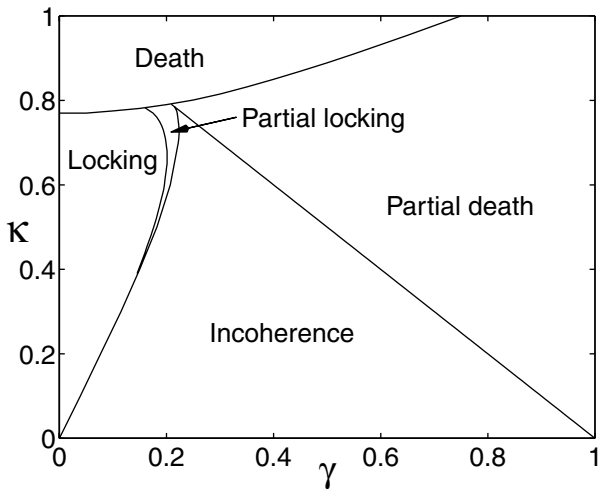

FIG. 3. Phase diagram for Eqs. (1) and (2), assuming a uniform distribution of natural frequencies on $[1-\gamma, 1+\gamma]$. The boundary between locking and partial locking is determined numerically; all other boundaries are determined analytically. All of the partially locked hybrid states are lumped together in one region, for simplicity.

We now outline our analytical calculations of the boundaries of the regions corresponding to incoherence, partial death, and death. Following the standard approach used for the Kuramoto model [2–4], we rewrite the dynamics in the infinite-N limit. For each frequency ω, let $p(\theta, t, \omega)$ denote the density of oscillators at phase θ at time t, and let $v(\theta, t, \omega)$ denote the local velocity field. Then p satisfies the continuity equation $\partial p/\partial t = -\partial(pv)/\partial\theta$, expressing conservation of oscillators of frequency ω. The velocity v is determined by applying the law of large numbers to Eq. (1); the sum over all oscillators in (1) is replaced by an integral as $N \to \infty$, yielding $v(\theta, t, \omega) = \omega - \sigma(t)\sin\theta$, where

$$\sigma(t) = \kappa \int_0^{2\pi} \int_{1-\gamma}^{1+\gamma} (1 + \cos\theta) p(\theta, t, \omega) g(\omega)\, d\omega\, d\theta\,. \tag{3}$$

Additionally, we demand that p be nonnegative, 2π-periodic in θ, and we impose the normalization $\int_0^{2\pi} p(\theta, t, \omega)\, d\theta = 1$ for all t, ω.

The key to the analysis is recognizing that incoherence, partial death, and death correspond to *stationary* densities $p_0(\theta, \omega)$ in the infinite-N limit. Hence, one may solve for all three states by seeking fixed points of the continuity equation; these satisfy $p_0 v_0 = C(\omega)$, with $C(\omega)$ determined by normalization. Depending on its natural frequency, an oscillator's steady-state behavior falls into one of two categories. (i) $\omega \le \sigma$: In this case, $v_0 = \omega - \sigma\sin\theta = 0$. The oscillators of a given frequency $\omega \le \sigma$ all remain stuck at a single phase $\theta^*(\omega)$, defined implicitly by $\sin\theta^* = \omega/\sigma$. Their density is $p_0(\theta, \omega) = \delta[\theta - \theta^*(\omega)]$. Such oscillators are motionless, or dead. (ii) $\omega > \sigma$: These oscillators rotate nonuniformly around the circle, hesitating near $\theta = \pi/2$ and accelerating near $\theta = 3\pi/2$, as dictated by their velocity field $v_0 = \omega - \sigma\sin\theta > 0$. Although individual oscillators are moving, their number density is stationary. The fixed point condition implies that the density is inversely proportional to the velocity:

$$p_0(\theta, \omega) = \frac{C(\omega)}{\omega - \sigma\sin\theta}\,. \tag{4}$$

Normalization then determines $C(\omega) = \sqrt{\omega^2 - \sigma^2}/(2\pi)$. From these two basic scenarios, we are able to calculate the incoherence, partial death, and death boundaries as follows.

Incoherence exists provided $\omega > \sigma$ for all ω; then all oscillators belong to category (ii) above. The boundary separating incoherence and partial death occurs when $\sigma = \omega_{\min}$, where $\omega_{\min} = 1 - \gamma$. The first oscillators to die are the slowest ones. To solve for σ, we substitute (4) into Eq. (3); this yields $\sigma = \kappa$. Thus, partial death bifurcates from incoherence along the straight line

$$\kappa = 1 - \gamma\,, \tag{5}$$

assuming κ is not so large that the system is in the death region. Remarkably, this result holds for any frequency distribution $g(\omega)$, whether symmetric or not.

The stability of the incoherent state is determined by linearizing the continuity equation about the incoherent density (4). The resulting linear operator has a continuous spectrum that is pure imaginary and a discrete spectrum that is governed by the equation [17]

$$\kappa = \int_{1-\gamma}^{1+\gamma} \frac{\lambda\omega(\omega - \sqrt{\omega^2 - \kappa^2})}{\lambda^2 + \omega^2 - \kappa^2}\, g(\omega)\, d\omega\,. \tag{6}$$

From (6), it is clear there are no eigenvalues λ with $\mathrm{Re}(\lambda) < 0$; if there were, the right-hand side would have negative real part, contradicting the assumption $\kappa \ge 0$. Thus, incoherence is either unstable or neutrally stable. Numerics indicate that the boundary between incoherence and partial locking corresponds to a Hopf bifurcation. To obtain the boundary, we solve Eq. (6) for λ perturbatively, assuming $\gamma \ll 1$, and then take the limit $\mathrm{Re}(\lambda) \to 0^+$. The result for a uniform $g(\omega)$ is

$$\kappa = \frac{8\gamma}{\pi}\left[1 + \frac{16\gamma^2}{\pi^2} + \frac{16(\pi^2 + 80)\gamma^4}{\pi^4}\right] + O(\gamma^7)\,. \tag{7}$$

This formula agrees with numerical simulations to within 4% for $\kappa \le 0.6$. In the limit $\gamma \to 0$, Eq. (7) reduces to $\kappa = 8\gamma/\pi$, which is the critical coupling threshold for the averaged system (the Kuramoto model, with coupling $K = \kappa/2$). Hence, Eq. (7) can be viewed as an extension of the classical threshold condition [1,2] into the nonaveraged regime of stronger coupling and frequency disorder.

Finally, to calculate the death boundary we use a self-consistency argument familiar from mean-field theory [2]. In the death state, each oscillator comes to rest at $\theta^*(\omega)$, defined by the zero velocity condition $\sin\theta^* = \omega/\sigma$. This requires $\sigma \ge \omega_{\max}$, where $\omega_{\max} = 1 + \gamma$. Each phase

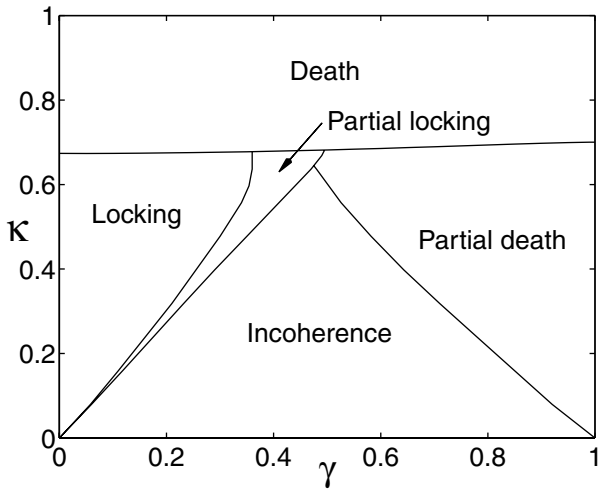

FIG. 4. Phase diagram for (1) with $R(\theta)$ as in (2), $P(\theta) = a_n(1 + \cos\theta)^n$, $n = 10$, and a uniform frequency distribution on $[1 - \gamma, 1 + \gamma]$. Death boundary determined analytically; all other boundaries determined numerically.

$\theta^*(\omega)$ depends on σ, which in turn depends on all phases via Eq. (3); therefore, σ must be determined self-consistently. For each ω, there are two possible roots $\theta^*(\omega)$: one in $[0, \pi/2]$, the other in $[\pi/2, \pi]$. The unique stable fixed point of Eq. (1) satisfies $0 \le \theta^*(\omega) \le \pi/2$ for all ω. Putting the corresponding density $p_0(\theta, \omega) = \delta[\theta - \theta^*(\omega)]$ into Eq. (3) gives the self-consistency condition

$$\frac{\sigma}{\kappa} = 1 + \int_{1-\gamma}^{1+\gamma} \sqrt{1 - \left(\frac{\omega}{\sigma}\right)^2}\, g(\omega)\, d\omega\,. \qquad (8)$$

In order for death to exist, there must be a root $\sigma \ge 1 + \gamma$ of Eq. (8). The boundary between death and partial death corresponds to an end point bifurcation, and is found by setting $\sigma = 1 + \gamma$ in (8). For a uniform $g(\omega)$ this yields the exact expression

$$\frac{1}{\kappa} = \frac{1}{4\gamma}\left[2 + \frac{\pi}{2} - \Delta(2 + \sqrt{1 - \Delta^2}) - \sin^{-1}\Delta\right], \qquad (9)$$

where $\Delta = (1 - \gamma)/(1 + \gamma)$. The remaining portion of the boundary, separating death from full and partial locking, corresponds to a saddle-node bifurcation. It is obtained by solving Eq. (8) numerically, along with the tangency condition $1/\kappa = F'(\sigma)$, where $F(\sigma)$ is the right-hand side of Eq. (8).

To test the robustness of the phase diagram, we replaced $P(\theta)$ in (2) with a family of influence functions $P_n(\theta) = a_n(1 + \cos\theta)^n$, $n \ge 1$ which becomes more and more sharply peaked as n increases. [The normalization coefficients a_n are determined by requiring $P_n(\theta)$ to have integral equal to 2π over one cycle. Note that $P_n(\theta) \to 2\pi\delta(\theta)$ as $n \to \infty$.] We find that all of the phenomena observed for the model studied in this paper ($n = 1$) persist as we increase n. The only difference is that the boundaries become slightly distorted [Fig. 4].

The mean-field model (1) is one of the simplest models of pulse-coupled oscillators. More realistic models would incorporate features such as spatial coupling, time delay, dynamical synapses, refractory period, non-sinusoidal influence and sensitivity functions, etc. It remains to be seen whether such models would exhibit additional states beyond those found here. In any case, we now know that even the most idealized version of the Winfree model displays a fascinating wealth of dynamics that, curiously, escaped notice for over thirty years.

Research was supported in part by the National Science Foundation.

[1] A. T. Winfree, J. Theor. Biol. **16**, 15 (1967).
[2] Y. Kuramoto, *Chemical Oscillations, Waves, and Turbulence* (Springer, Berlin, 1984).
[3] Y. Kuramoto and I. Nishikawa, J. Stat. Phys. **49**, 569 (1987); S. H. Strogatz and R. E. Mirollo, J. Stat. Phys. **63**, 613 (1991); L. L. Bonilla, J. C. Neu, and R. Spigler, J. Stat. Phys. **67**, 313 (1992); H. Daido, Phys. Rev. Lett. **73**, 760 (1994); J. D. Crawford, J. Stat. Phys. **74**, 1047 (1994).
[4] For a review of work on the Kuramoto model, see S. H. Strogatz, Physica (Amsterdam) **143D**, 1 (2000).
[5] K. Wiesenfeld, P. Colet, and S. H. Strogatz, Phys. Rev. E **57**, 1563 (1998).
[6] J. Pantaleone, Phys. Rev. D **58**, 073002 (1998).
[7] R. Häußler, R. Bartussek, and P. Hänggi, in *Applied Nonlinear Dynamics and Stochastic Systems near the Millennium,* edited by J. B. Kadtke and A. Bulsara, AIP Conf. Proc. No. 411 (AIP, New York, 1997), pp. 243–248.
[8] G. Russo and P. Smereka, SIAM J. Appl. Math. **56**, 327 (1996).
[9] G. Kozyreff, A. G. Vladimirov, and P. Mandel, Phys. Rev. Lett. **85**, 3809 (2000).
[10] S. H. Strogatz, R. E. Mirollo, and P. C. Matthews, Phys. Rev. Lett. **68**, 2730 (1992).
[11] R. E. Mirollo and S. H. Strogatz, SIAM J. Appl. Math. **50**, 1645 (1990); C. van Vreeswijk, L. F. Abbott, and G. B. Ermentrout, J. Comp. Neurol. **1**, 313 (1994); A. V. M. Herz and J. J. Hopfield, Phys. Rev. Lett. **75**, 1222 (1995); W. Gerstner, J. L. van Hemmen, and J. D. Cowan, Neural Comput. **8**, 1653 (1996); P. C. Bressloff and S. Coombes, Phys. Rev. Lett. **81**, 2168 (1998); C. C. Chow, Physica (Amsterdam) **118D**, 343 (1998); D. Golomb and D. Hansel, Neural Comput. **12**, 1095 (2000).
[12] G. B. Ermentrout and N. Kopell, SIAM J. Appl. Math. **50**, 125 (1990).
[13] J. Buck, Q. Rev. Biol. **63**, 265 (1988).
[14] A. T. Winfree, *The Geometry of Biological Time* (Springer, New York, 1980).
[15] For examples of phase-response curves that are approximately sinusoidal, see Fig. 4 in Ref. [13] and Figs. 5–7, pp. 414–417 in Ref. [14].
[16] P. S. G. Stein, J. Neurophysiol. **34**, 310 (1971).
[17] J. T. Ariaratnam and S. H. Strogatz (to be published).